

Attachment, Proliferation and Differentiation of Mesenchymal Stem Cells on Implant Coated with Chitosan

Banna M Al-Nufaiy¹ and Khalid S Al-Hamdan²

¹ Resident Periodontics Graduate Program, Department of Periodontics College of Dentistry King Saud University, PO Box;124202, Riyadh, Saudi Arabia.

²Diplomate, American Board of Periodontology, Associate Professor Department of Periodontics College of Dentistry King Saud University, PO Box;7669 King Saud University Unite-1 /12372 Riyadh, Saudi Arabia.

ABSTRACT

Osteogenesis is characterized by a serial of events involving cells attachment, proliferation, and differentiation. However, chitosan applications in osteogenesis mechanisms have remained limited. This study intends to examine chitosan's effect with different degrees of deacetylation (DDA) as a coating material for the Resorbable Blast Textured (RBT) implant surface. 63 Resorbable Blast Textured discs were coated either with 80 or 95 DDA. These discs were categorized into three groups i.e., RBT 80, RBT 95, and RBT control (without coating). After their separate applications, Cell viability, morphology, and bone formation were studied at 7 and 14 days. All samples showed biocompatibility and allowed cell attachment. However, areas with high cellular density were found in abundance around surfaces coated with chitosan in comparison with the control. At day 14, test groups coated with chitosan, especially 95 DDA, showed significant mineralization process and growth of nodule-like structures of hMSCs on the surfaces. No significant differences were found in cell viability except for RBT 80, which was lower in comparison to other groups. RBT 95 showed a significant increase in all osteoblast markers in comparison with RBT 80 and control. Chitosan material was confirmed as a right candidate for implant coated with Resorbable Blast Textured surface.

KEY WORDS: BONE CELL; CHITOSAN FILM; DEGREE OF DE-ACETYLATION, IMPLANT COATING.

INTRODUCTION

It is well recognized that functional allogenic tissue development necessitates the coordination of cell adhesion, growth, differentiation, and organization into a particular tissue architecture (Rogina et al.,

2017). Similarly, the development of the stem cell microenvironment has become critical for regenerative medicine (Bardelli and Moccetti, 2017). Studies show mesenchymal stem cells (MSCs), which are isolated from the adult bone marrow, possess self-renewing capability which able to differentiate into various cell phenotypes, showing their potential beneficial use for bone tissue regeneration. Concerning the implant therapies, various studies show functional as well as biological advantages for the patients in contrast to the conventional method, providing benefits in the long-run. This is evident from the ten years long study with survival and success rate of 95 percent (Buser et al., 2012; Fischer and Stenberg, 2012, Li et al., 2016, Mora et al., 2017).

ARTICLE INFORMATION

*Corresponding Author: khalidh1@ksu.edu.sa

Received 10th July 2020 Accepted after revision 26th Sep 2020

Print ISSN: 0974-6455 Online ISSN: 2321-4007 CODEN: BBRCBA

Thomson Reuters ISI Web of Science Clarivate Analytics USA and Crossref Indexed Journal



NAAS Journal Score 2020 (4.31) SJIF: 2020 (7.728)

A Society of Science and Nature Publication,

Bhopal India 2020. All rights reserved

Online Contents Available at: <http://www.bbrc.in/>

DOI: <http://dx.doi.org/10.21786/bbrc/13.3/93>

Mainly, the success of the implantation depends on osseointegration, which constitutes bone modeling and remodeling processes (Li et al., 2018). Optimal osseointegration depends on the material implant characteristics, implant loading, and surgical techniques as well as the quality, distribution, and amount of bone present at the implant insertion site (Guglielmotti et al., 2019, Chen et al., 2019). Accelerating this process is a modern trend in implant dentistry, which relevance increases when treating medically compromised patients such as diabetic and osteoporotic patients (Naujokat et al., 2016, Vohra et al., 2014). To minimize the treatment time, the implant surface coating of the biomimetic materials or agents is used. In this regard, increased use of chitosan (CH), a natural biocompatible polysaccharide derived from the crustacean shells, has been observed (Elieh-Ali-Komi and Hamblin, 2016). Chitosan comprises various polymers with a varying differences in molecular weight, degree of deacetylation (DDA), and viscosity (Kumaran, 2020).

Su et al., (2017) have reported an increasing level of resemblance between the bone and cartilages extracellular matrix and CH components and chemical structure. Arunkumar et al. (2017) showed that CH components also denotes effective osteoconductivity, which help improve the vitro as well as vivo tissue generation (Arunkumar et al., 2017). Other biological properties have been indicated by previous searches on CH include antitumor, antioxidant, and antimicrobial characteristics (Pippi et al., 2017, Costa et al., 2014, Cheung et al., 2015). However, these properties are likely to be affected by DDA, which refers to the deacetylated units' molar fraction or deacetylation percentage and the molar weight of CH (Jiang et al., 2017). Most studies highlight the impact of chemical and physical properties of DDA on CH as a coating material (Cheung et al., 2015; Bumgardner et al., 2007). For instance, one study revealed that different DDA of chitosan as implant coating did not affect the cell growth nor the degradation rate. However, the tensile bond strength was lower, with 81.7% DDA (Yuan et al., 2008). However, Limited studies have focused on the effect of DDA on chitosan coating potential.

Although chitosan has been approved to be an excellent coating material and was investigated using different in vitro/vivo models (Govindharajulu et al., 2017, Husain et al., 2017), previous studies were focused on coating a commercially pure titanium surface, and no study used different surfaces to test the coating potential. Therefore, the aim of this investigation was to determine the morphology, proliferation, and pattern of attachment of hMSC-TERT 20 on chitosan with two degrees of deacetylation (DDA) as a coating material for Resorbable Blast Textured implant surface (RBT).

MATERIAL AND METHODS

Materials: The powdered form of chitosan of about 200 kDa molecular mass and 500 mPas viscosity with two different DDA 80 and 95 were used (Heppe Medical

Chitosan GmbH, Germany). 63 Textured implant surface (RBT) discs with a diameter of 10 mm (Biohorizon company) were utilized. The discs were divided into three groups with 21 discs for each: RBT 80, RBT 95, and RBT control.

Coating Procedure: The chemical bond between the CH material and the disc surface was created through a silanization reaction adapted from Bumgardner et al. methodology with some modification (Bumgardner et al., 2003b). Briefly, the disc surfaces were suspended in water/ethanol solution (5:95 vol %) acidifying to 4.5 pH and 10 M acetic acid. Following it, 2 vol% silane-coupling agent was added for ten minutes at room temperature, whereas pH level was sustained at 4.5 to 5.5. The non-adhered silane was removed by rinsing the disc with ethanol and was cured at $110 \pm C$. Then, the implanted disc was suspended overnight in glutaraldehyde solution (2 vol %), with a pH of 4.3 at room temperature. After this, a solution of CH (2 wt. %) was prepared with acetic acid (0.2%) at room temperature.

For eliminating the undissolved particles, the CH was centrifuged before casting. Later, the chitosan was kept at $4^{\circ}C$ overnight. Next, the disc was cast with CH solution of 1ml at room temperature. Water was allowed to evaporate over 5-7 days. After coating and before seeding, 1 disc from each group was studied under the scanning electron microscopy (SEM). Implant coated with chitosan were sterilized using ultraviolet (UVUV) light for an hour followed by ethanol soaking (70%) for two hours, and then it was washed using Phosphate Buffer Saline (PBS) twice (Govindharajulu et al., 2017, Abuelreich et al., 2017).

Cell Culture: Both coated and non-coated discs were placed in individual wells. For human bone marrow-derived mesenchymal stem cells (hBM-MSCs), hMSC-TERT 20 passage 54 were used. The cell growth occurred in a media which consist of DMEM (ATCC, Manassa, VA, USA) supplemented with 10% Fetal Bovine Serum (FBS), Penicillin-Streptomycin solution, 100X (10,000 Units/ml Penicillin +10,000 µg/ml Streptomycin) and 1% MEM Non-Essential Amino Acids Solution 10mM (100X, Cat No RMNAA-0100X) under standard cell culture conditions ($37^{\circ}C$, 100% humidity, 95% air, and 5% CO₂). Following 80-95% of cells confluence, they were collected, washed, and counted with a hemocytometer. The study used 1×10^6 cells, which were plated with culture medium onto implant discs and incubated for 24h to facilitate adherence to the surface.

After that, the media was changed for each implant disc and the cells were grown and maintained in an osteogenic medium which comprised of 100 nmol/L dexamethasone (Sigma-Aldrich, Cat No D1756-1G), 10 mmol/L Sodium β -glycerophosphate pentahydrate (Loba Chemie Ltd., India, Cat No 05885), 50 g/ml L-Ascorbic Acid, Vitamin C (Winlab Ltd., UK, Cat No 107888), and Cholecalciferol, (+)-Vitamin D3 (Cat No C9756-1G). The media was changed every three days.

Cell Viability Assays: AlamarBlue (ABAB) assay was used to evaluate the cell viability (AbD Serotec, Raleigh, NC, USA). For each reaction, 10 % of Alamar blue was diluted into 100 µl of DMEM and incubated in the dark for 60 minutes at 37°C. The samples were read through a microplate reader (Synergy™ 2 Multi-Mode Microplate Reader) at 590 nm. Three readings were recorded for each sample at each time point.

Quantitative Real-Time-Polymerase Chain Reaction (qPCR): RNA isolation was accomplished at days 7 and 14 using recommended BIOFACT HiGene Total RNA Prep Kit (Biofact, Cat No RP101-100, Korea). RNA concentration and protein contamination were measured using a spectrophotometer (Eppendorf-Biospectrometer basic). Samples with ratios between 1.8 and 2.0 purity were used. Amplification and synthesis of Complementary DNA (cDNA) was done from 1µg of RNA using a FIREScript RT cDNA synthesis KIT (Solis BioDyne, Cat No 06-15-00200). Using a total reaction volume of 20µl and HOT FIREPol® EvaGreen® qPCR Supermix (Solis BioDyne, Cat No 08-36-00008), QPCR were completed. For normalization, B-actin was added for all the reactions as a control gene. All qPCR assays were performed and accomplished under the same conditions as triplicate (n=10, duplicate independent experiments). The primers' sense and antisense were designed based on GenBank. The primers used in this experiment are listed in Table (1).

Table 1. Primers Sequence

Sequence Name	Description
OSTEONECTIN F	5' GAG GAA ACC GAA GAG G 3'
OSTEONECTIN R	5' GGG GTG TTG TTC TCA TCC AG 3'
RUNX2 F-RO	5' GTA GAT GGA CCT CGG GAA CC 3'
RUNX2 R-RO	5' GAG GCG GTC AGA GAA CAA AC 3'
OSTEOCALCIN R-RO	5' CTC ACA CAC CTC CCT G 3'
OSTEOCALCIN F-RO	5' GGC AGC GAG GTA GTG AAG AG 3'
ACTB (Beta-actin) R	5' ACATCTGCTGGA AGGTGGACA 3'
ACTB (Beta-actin) F	5' TCAAGATCATTGC TCCTCCTGAG 3'
ALPL F	5' GACGGACCCTC GCCAGTGCT 3'
ALPL R	5' AATCGACGTGGG TGGGAGGGG 3'

Measurement of Osteoblast Differentiation by Alkaline Phosphatase Activity: The alkaline phosphatase activity was measured quantitatively by using the Alkaline Phosphatase Activity Colorimetric Assay kit (BioVision, Cat No K412 -500ASSAY). In brief, after the induction

of cells on 7th and 14th day, the culture medium was removed and washed thrice using PBS. The cells were collected from the wells through trypsinization using 25% trypsin and afterward, centrifuged at 7500 rpm for 5 minutes. Next, the harvested cell pellet was treated by the kit while following the company's instruction manual. At 405 nm, the absorbance was measured in the microplate reader.

Cell Morphology: Scanning Electron Microscopy (SEM) was used for the examination of the cell culture at time intervals of 7 and 14 days. Before observation, the PBS was used to wash the implant discs thrice for eliminating all non-adherent cells and fixed in 4% v/v glutaraldehyde at 4°C overnight. Followed by the gradual immersion of the sample in water-ethanol solution. For osteoblast adhesion, Rhodamine-phalloidin staining was used to view the cellular actin filaments. After incubation of cells for 24hs, 4.0% paraformaldehyde was used to fix the samples for 15 minutes. Next, the cells were blocked by using 1.0% BSA for 30 minutes and then kept overnight at RT. The next day, the samples were stained for 30 minutes with 40, 60-diamidino-2-phenylindole (DAPI, Sigma, St. Louis, MO). The confocal microscope was used to obtain the fluorescence images (a Zeiss LSM510 META confocal system, connected to an inverted Zeiss Axiovert 200 microscope).

Ethical Approval: The study protocols, as outlined by the Kind Saud University Approval of the Ethical Board Committee, were followed. Institutional Review Board (No E-18-2850) as well as Dentistry Research Center (CDRC No. PR 0074) provided ethical consideration. The Molecular and Cell Biology Laboratory provided the hMSC-TERT20 in collaboration with Prince Naif Bin Abdulaziz Health Research Center.

Statistical Analysis: IBM SPSS (Statistical Package for Social Sciences/ SPSS 22; IBM Corp., NEW YORK, NY, USA) was used for the analysis of the results. The normality of the data was assessed by using the Shapiro-Wilk test. The statistical significance between groups were determined by using a two-way analysis of variance (ANOVA) followed by one-way analysis of variance (ANOVA) and the Tuckey post hoc assessment. Mean, and the standard deviation was computed for the measurable data. The significance value was determined at $P \leq 0.05$.

RESULTS AND DISCUSSION

The structural and chemical properties of chitosan make it an excellent alternative to traditional coating materials such as calcium phosphate (van Oirschot et al., 2016). This is consistent with the previous studies which considered chitosan as an osteoinductive material which can act as antimicrobial, accelerate wound healing, and can promote bone formation (Li et al., 2015, Pippi et al., 2017). The objective of this project was to determine the behavior of hMSC on implants with rough topography. To evaluate cell viability and attachment, the Resorbable Blast Textured implant surface was coated with chitosan

with two different DDAs. First of all, the coating architecture was studied under SEM for all groups. At a magnification of 1000, RBT control surface demonstrated multiple irregularities with small flaws, depressions, and spikes (Figure 1).

Figure 1: (a) gross view of Resorbable Blast Textured (RBT) surface without coating, (b) under SEM. (c) RBT surface coated with chitosan 80 DDA, (d) under SEM. (E) RBT surface coated with chitosan 95 DDA, (E) under SEM. All of the samples at a magnification of 1,000

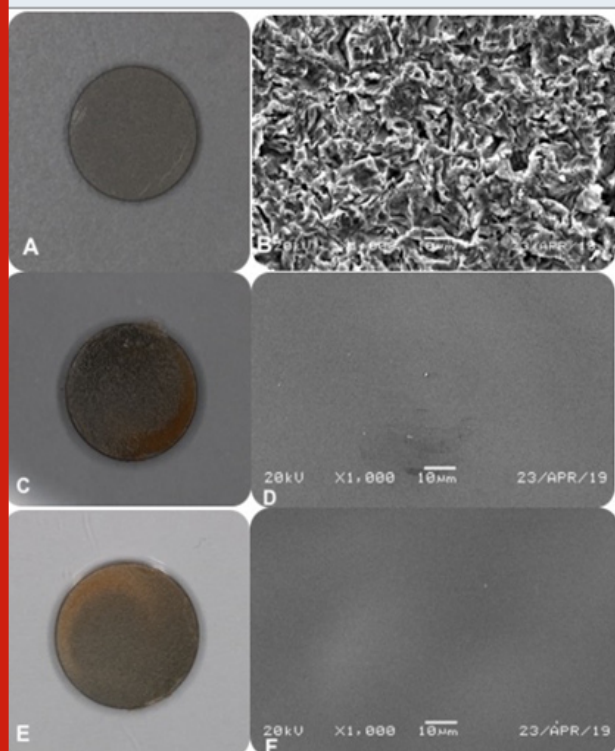
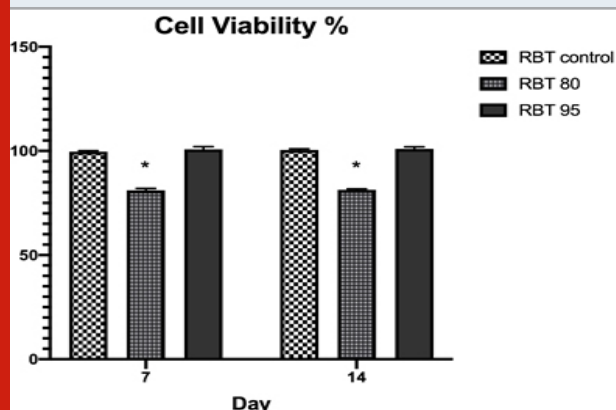


Figure 2: Alamar blue quantification for cell viability performed on cells grown on control or chitosan 80/95 coated groups during osteogenic differentiation for 7 and 14 days. Values were presented as mean \pm SDSD of six different groups. * $p < 0.05$



For chitosan 80 or 95 DDA, all of them showed a similar appearance in which they formed a homogenous and transparent coating, which is free from any cracks. The chitosan molecules chain was attached to the disc surface by their NH₂ groups. This attachment occurred through their silane-glutaraldehyde molecules, which account for the yellowish tint on all the coating (Yuan et al., 2008). Studies demonstrated that the silanization method is not only simple and cost-effective but also chemically binds the substrate to the implant surface, which confirmed by mechanical tests (Yuan et al., 2008, Bumgardner et al., 2003b).

The AlamarBlue results showed that no significant difference in cell viability between control and RBT 95 during day 7 and day 14 (Figure 2). However, RBT 80 was significantly lower in cellular viability at both time intervals in comparison with the other groups. This indicates that these surfaces were biocompatible and would not be cytotoxic in vivo, even with time progress. However, even though proliferation was lower in RBT 80, still full confluent cell layer and attachment were obtained at 7 and 14 days. Also, according to the International Organization ISO10993-5, if the cell viability remained >70%, then the material does not have cytotoxicity potentials (10993-5, 2009). One study found that cell attachment and proliferation was increased by chitosan with high DDA membranes which coated with fibronectin (Lieder et al., 2012).

This is different from the study findings of Abuelreich et al., which showed that cells cultured on the Chitosan-Polycaprolactone membrane had more cell attachment and less proliferation than plastic surface control (Abuelreich et al., 2017). Another study showed that keratinocyte was increased in proliferation when the DDA decreases; thus lower DDA will increase the cell adhesion. On the contrary, fibroblast demonstrated a better adhesion than keratinocyte, although they remain alive, they do not proliferate well regardless of the DDA. This kind of cell behavior was related to the high adhesion to the underline surface in which inhibits their growth (Chatelet et al., 2001). After that, the capacity of osteoblast cell growth was studied by using molecular assays.

Coated and non-coated samples were evaluated for the expression of Runx2, ALP, and matrix mineralization. Cells grown on chitosan-coated material have more expression of bone markers in comparison with the control group. Moreover, 95 DDA caused statistically higher bone marker expression than the other groups (Figure 3). Alkaline phosphatase (ALP) expression is the most commonly used marker for bone formation (Choi et al., 2011). Chitosan material influenced ALP activity at 7 and 14 days from cell culture with the highest activity on 95 DDA (Figure 3-4). The quantity of ALP enzyme was significantly lower in RBT control in comparison with the other groups. One study found that after 8 days of incubation, ALP's intracellular activity was higher on chitosan-coated titanium discs compared with the

pure titanium group. However, they used a combination between 85 and 90 DDA (Li et al., 2015).

Figure (3): Osteoblast gene expression at 7 and 14 days from cell culture.

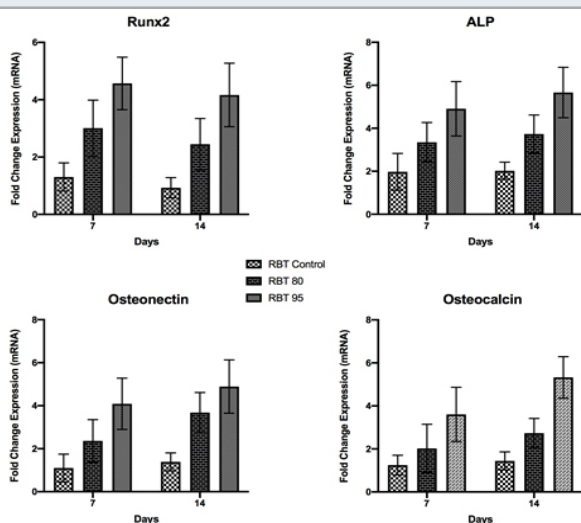
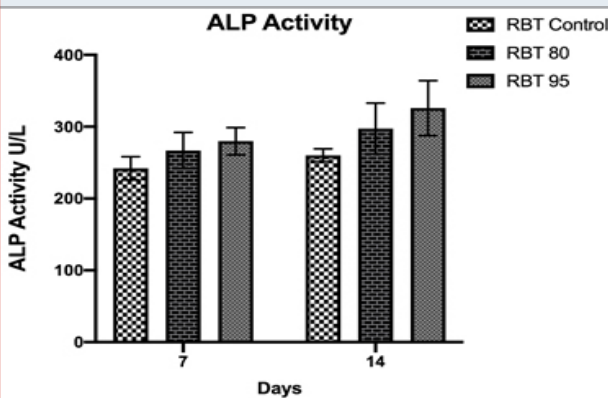


Figure 4: Alkaline phosphatase activity at 7 and 14 days of cell culture



Mineralization process can be detected by measuring the amount of Osteocalcin (OC) and Osteonectin (ON) activity (Ozdemir et al., 2016; Rosset and Bradshaw, 2016). The expression of these two non-collagenous markers increases in the final phases of bone formation by mature osteoblasts. Our data displayed that these genes were expressed more in chitosan-coated samples in comparison with the RBT control, and by following the general trend of bone mineralization, the expression of ON and OC was more at day 14 in comparison with day 7. A study by Mathews et al. examined different densities of chitosan with >87.61 DDA coating for osteoblast differentiation. Chitosan coated plates revealed more gene expression of osteoblast markers, including Runx2, ALP, ON, OC on day 7, 14 and 21 from cell culture in comparison with untreated plates. Moreover, calcium deposition measured by quantification assay was 30% more on chitosan-coated plates by day 14 and 21 from osteogenic induction (Mathews et al., 2011).

Figure 5: (G-L) Scanning electron microscopy (SEM) images. (G) RBT control at day 7 (H) at day 14. (I) RBT 80 at day 7 (J) at day 14. (K) RBT 95 at day 7. (L) At day 14. 2500× magnification.

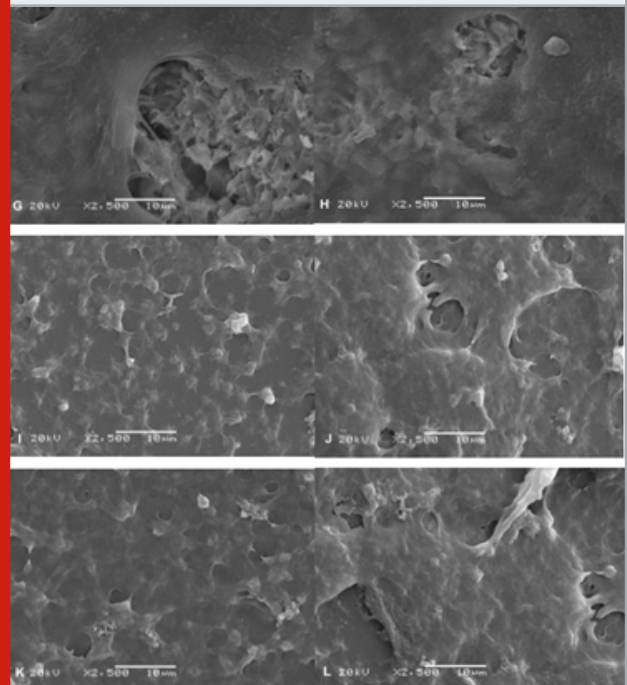
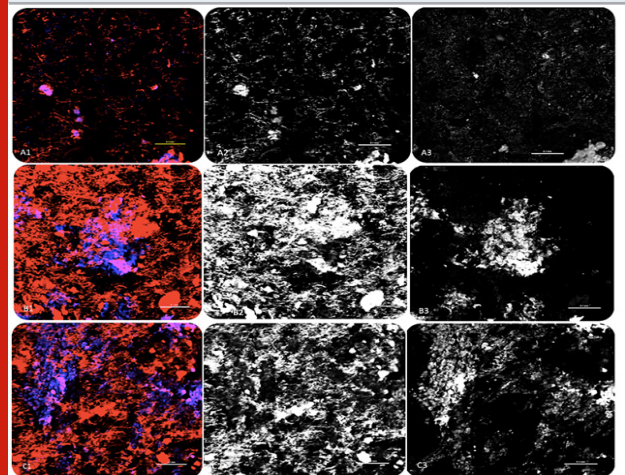


Figure (6): Images of cell morphology and osteoblast adhesion. (A1) for RBT control as all. (A2) with Phalloidin for actin filaments. (A3) nuclei stained with DAPI. (B1) for RBT 80 as all. (B2) with Phalloidin for actin filaments. (B3) nuclei stained with DAPI. (C1) for RBT 95 as all. (C2) with Phalloidin for actin filaments. (C3) nuclei stained with DAPI.



According to the literature, the deacetylation degree in the chitosan is high with an increased number of amino groups, which is better for implant surface bonding. Thereby, an increase in the amino group is likely to increase the positively charged particles, which leads to a high net positive charge on the coated samples. Consequently, the coating will have a higher affinity for

negatively-charged cells and growth factors (Bumgardner et al., 2003a, Hamilton et al., 2007, Prasitsilp et al., 2000, Fakhry et al., 2004). Overall, all surfaces showed good biocompatibility and allowed for cell attachment, proliferation, and differentiation. After 24 h, the confocal results indicated that hMSC could attach and grow on chitosan-coated surfaces as well as control.

For RBT 95 and RBT 80, dense flattened osteoblasts approximating each other were seen on the top of the surface (Figure 6). For SEM results, the samples coated with chitosan showed more layers of dark cell patches overlapping each other while forming bridge-like structure at day 7 (Figure 5). With a later stage, the calcium deposits were clearly visible at the chitosan-coated groups in contrast to the control groups. The nodule-like structures suggested that the cells were committed to developing osteogenic phenotype and osteoblasts differentiation (Abuelreich et al., 2017).

Concerning the different DDAs, the results of the present study showed that 95 DDA coated chitosan is superior in terms of biological responses in comparison with 80 DDA coated chitosan. Research by Foster and his group showed that cell line, which grew on 85 DDA was much better in cell spreading in comparison with 72 DDA (Foster et al., 2015). On the contrary, A recent study investigated the influence of DDA on the biological behavior of the MC3T3-E1 cells and found that a DDA in the range of 87–94% had a less critical effect on cell growth or proliferation in comparison with the source of chitin (shrimp & crabs) (Supernak-Marczewska and Zielinski, 2020). To the best of the researcher's knowledge, this is the first study that utilized chitosan to coat implant surface other than pure titanium, and these data encourage future researchers to do more investigation regarding the mechanical properties of this combination for future implant design.

ACKNOWLEDGMENTS

This research project was funded by Prince Naif Bin Abdulaziz Health Research Center (No245843), King Saud University Medical City, Riyadh. Also, The hMSC-TERT20 line was kindly provided by the Molecular and Cell Biology Laboratory, College of Dentistry, in collaboration with the Prince Naif Bin Abdulaziz Health Research Center. The integrated content is the sole responsibility of the authors and cannot be considered as an official outlook of the Prince Naif Bin Abdulaziz Health Research Center or the KSU Medical City Also, we thanks Biohorizon company for providing us with the implant discs..

Conflicts of Interest: This study has no conflicts of interest.

REFERENCES

Abuelreich, S., Manikandan, M., Aldahmash, A., Alfayez, M., Al Rez, M. F., Fouad, H., Hashem, M., Ansari, S. G., Al-Jassir, F. F. & Mahmood, A. 2017. Human Bone

Marrow Mscs Form Cartilage And Mineralized Tissue On Chitosan/Polycaprolactone (Cs/Pcl) Combined Nanofibrous Scaffolds. *Journal Of Nanoscience And Nanotechnology*, 17, 1771-1778.

Arunkumar, P., Indulekha, S., Vijayalakshmi, S. & Srivastava, R. 2016. Poly (Caprolactone) Microparticles And Chitosan Thermogels Based Injectable Formulation Of Etoricoxib For The Potential Treatment Of Osteoarthritis. *Mater Sci Eng C Mater Biol Appl*, 61, 534-44.

Bardelli, S. & Moccetti, M. 2017. Remodeling The Human Adult Stem Cell Niche For Regenerative Medicine Applications. *Stem Cells International*, 2017, 6406025-6406025.

Bumgardner, J. D., Chesnutt, B. M., Yuan, Y., Yang, Y., Appleford, M., Oh, S., McLaughlin, R., Elder, S. H. & Ong, J. L. 2007. The Integration Of Chitosan-Coated Titanium In Bone: An In Vivo Study In Rabbits. *Implant Dent*, 16, 66-79.

Bumgardner, J. D., Wiser, R., Elder, S. H., Jouett, R., Yang, Y. & Ong, J. L. 2003a. Contact Angle, Protein Adsorption And Osteoblast Precursor Cell Attachment To Chitosan Coatings Bonded To Titanium. *J Biomater Sci Polym Ed*, 14, 1401-9.

Bumgardner, J. D., Wiser, R., Gerard, P. D., Bergin, P., Chestnutt, B., Marin, M., Ramsey, V., Elder, S. H. & Gilbert, J. A. 2003b. Chitosan: Potential Use As A Bioactive Coating For Orthopaedic And Craniofacial/ Dental Implants. *J Biomater Sci Polym Ed*, 14, 423-38.

Buser, D., Janner, S. F., Wittneben, J. G., Bragger, U., Ramseier, C. A. & Salvi, G. E. 2012. 10-Year Survival And Success Rates Of 511 Titanium Implants With A Sandblasted And Acid-Etched Surface: A Retrospective Study In 303 Partially Edentulous Patients. *Clin Implant Dent Relat Res*, 14, 839-51.

Chatelet, C., Damour, O. & Domard, A. 2001. Influence Of The Degree Of Acetylation On Some Biological Properties Of Chitosan Films. *Biomaterials*, 22, 261-8.

Chen, J., Cai, M., Yang, J., Aldhohrah, T. & Wang, Y. 2019. Immediate Versus Early Or Conventional Loading Dental Implants With Fixed Prostheses: A Systematic Review And Meta-Analysis Of Randomized Controlled Clinical Trials. *The Journal Of Prosthetic Dentistry*, 122, 516-536.

Cheung, R. C., Ng, T. B., Wong, J. H. & Chan, W. Y. 2015. Chitosan: An Update On Potential Biomedical And Pharmaceutical Applications. *Mar Drugs*, 13, 5156-86.

Choi, M. H., Noh, W. C., Park, J. W., Lee, J. M. & Suh, J. Y. 2011. Gene Expression Pattern During Osteogenic

- Differentiation Of Human Periodontal Ligament Cells In Vitro. *J Periodontal Implant Sci*, 41, 167-75.
- Costa, E. M., Silva, S. & Pina, C. 2014. Antimicrobial Effect Of Chitosan Against Periodontal Pathogens Biofilms. *Soj Microbiol Infect Dis*, 2(1);, 6.
- Elieh-Ali-Komi, D. & Hamblin, M. R. 2016. Chitin And Chitosan: Production And Application Of Versatile Biomedical Nanomaterials. *Int J Adv Res (Indore)*, 4, 411-427.
- Fakhry, A., Schneider, G. B., Zaharias, R. & Senel, S. 2004. Chitosan Supports The Initial Attachment And Spreading Of Osteoblasts Preferentially Over Fibroblasts. *Biomaterials*, 25, 2075-9.
- Fischer, K. & Stenberg, T. 2012. Prospective 10-Year Cohort Study Based On A Randomized Controlled Trial (Rct) On Implant-Supported Full-Arch Maxillary Prostheses. Part 1: Sandblasted And Acid-Etched Implants And Mucosal Tissue. *Clin Implant Dent Relat Res*, 14, 808-15.
- Foster, L. J., Ho, S., Hook, J., Basuki, M. & Marcal, H. 2015. Chitosan As A Biomaterial: Influence Of Degree Of Deacetylation On Its Physiochemical, Material And Biological Properties. *Plos One*, 10, E0135153.
- Govindharajulu, J. P., Chen, X., Li, Y., Rodriguez-Cabello, J. C., Battacharya, M. & Aparicio, C. 2017. Chitosan-Recombinamer Layer-By-Layer Coatings For Multifunctional Implants. *Int J Mol Sci*, 18.
- Guglielmotti, M. B., Olmedo, D. G. & Cabrini, R. L. 2019. Research On Implants And Osseointegration. *Periodontology 2000*, 79, 178-189.
- Hamilton, V., Yuan, Y., Rigney, D. A., Chesnutt, B. M., Puckett, A. D., Ong, J. L., Yang, Y., Haggard, W. O., Elder, S. H. & Bumgardner, J. D. 2007. Bone Cell Attachment And Growth On Well-Characterized Chitosan Films. *Polymer International*, 56, 641-647.
- Husain, S., Al-Samadani, K. H., Najeeb, S., Zafar, M. S., Khurshid, Z., Zohaib, S. & Qasim, S. B. 2017. Chitosan Biomaterials For Current And Potential Dental Applications. *Materials (Basel, Switzerland)*, 10, 602.
- Jiang, Y., Fu, C., Wu, S., Liu, G., Guo, J. & Su, Z. 2017. Determination Of The Deacetylation Degree Of Chitooligosaccharides. *Mar Drugs*, 15, 10993-5.
- I. 2009. Biological Evaluation Of Medical Devices. Part 5: Tests For In Vitro Cytotoxicity.
- Kumaran, S. A. W., Karthika, M., Anandajothi, E., Balaji, N. P., Pugazhvendan S. R., Rajeswari, V., Bharathi, S., Rajasekar, T., Prasad, S. G. 2020. Trends In Aquaculture Feed Development With Chitosan Nano Particles- A Review. *Biosci.Biotech.Res.Comm*, 13(1).
- Li, K., Kong, Y., Zhang, M., Xie, F., Liu, P. & Xu, S. 2016. Differentiation Of Pluripotent Stem Cells For Regenerative Medicine. *Biochem Biophys Res Commun*, 471, 1-4.
- Li, X., Ma, X. Y., Feng, Y. F., Ma, Z. S., Wang, J., Ma, T. C., Qi, W., Lei, W. & Wang, L. 2015. Osseointegration Of Chitosan Coated Porous Titanium Alloy Implant By Reactive Oxygen Species-Mediated Activation Of The Pi3k/Akt Pathway Under Diabetic Conditions. *Biomaterials*, 36, 44-54.
- Li, Z., Muller, R. & Ruffoni, D. 2018. Bone Remodeling And Mechanobiology Around Implants: Insights From Small Animal Imaging. *J Orthop Res*, 36, 584-593.
- Lieder, R., Darai, M., Thor, M. B., Ng, C. H., Einarsson, J. M., Gudmundsson, S., Helgason, B., Gaware, V. S., Masson, M., Gislason, J., Orlygsson, G. & Sigurjonsson, O. E. 2012. In Vitro Bioactivity Of Different Degree Of Deacetylation Chitosan, A Potential Coating Material For Titanium Implants. *J Biomed Mater Res A*, 100, 3392-9.
- Mathews, S., Gupta, P. K., Bhone, R. & Tote, S. 2011. Chitosan Enhances Mineralization During Osteoblast Differentiation Of Human Bone Marrow-Derived Mesenchymal Stem Cells, By Upregulating The Associated Genes. *Cell Proliferation*, 44, 537-549.
- Mora, C., Serzanti, M., Consiglio, A., Memo, M. & Dell'era, P. 2017. Clinical Potentials Of Human Pluripotent Stem Cells. *Cell Biol Toxicol*, 33, 351-360.
- Naujokat, H., Kunzendorf, B. & Wiltfang, J. 2016. Dental Implants And Diabetes Mellitus-A Systematic Review. *Int J Implant Dent*, 2, 5.
- Ozdemir, B., Kurtis, B., Tuter, G., Senguven, B. & Yildirim, B. 2016. Osteocalcin And Osteonectin Expression After Double Application Of Platelet-Rich Plasma In Rabbits. *Journal Of Istanbul University Faculty Of Dentistry*, 50, 1-9.
- Pippi, R., Santoro, M. & Cafolla, A. 2017. The Use Of A Chitosan-Derived Hemostatic Agent For Postextraction Bleeding Control In Patients On Antiplatelet Treatment. *J Oral Maxillofac Surg*.
- Prasitsilp, M., Jenwithisuk, R., Kongsuwan, K., Damrongchai, N. & Watts, P. 2000. Cellular Responses To Chitosan In Vitro: The Importance Of Deacetylation. *J Mater Sci Mater Med*, 11, 773-8.
- Rogina, A., Antunovic, M., Pribolsan, L., Caput Mihalic, K., Vukasovic, A., Ivkovic, A., Marijanovic, I., Gallego Ferrer, G., Ivankovic, M. & Ivankovic, H. 2017. Human Mesenchymal Stem Cells Differentiation Regulated By Hydroxyapatite Content Within Chitosan-Based Scaffolds Under Perfusion Conditions. *Polymers (Basel)*, 9.
- Rosset, E. M. & Bradshaw, A. D. 2016. Sparc/Osteonectin In Mineralized Tissue. *Matrix Biol*, 52-54, 78-87.

- Su, C. J., Tu, M. G., Wei, L. J., Hsu, T. T., Kao, C. T., Chen, T. H. & Huang, T. H. 2017. Calcium Silicate/Chitosan-Coated Electrospun Poly (Lactic Acid) Fibers For Bone Tissue Engineering. *Materials* (Basel), 10.
- Supernak-Marczewska, M. & Zielinski, A. 2020. Effects Of The Origin And Deacetylation Degree Of Chitosan On Properties Of Its Coatings On Titanium. *Coatings*, 10, 99.
- Van Oirschot, B. A., Bronkhorst, E. M., Van Den Beucken, J. J., Meijer, G. J., Jansen, J. A. & Junker, R. 2016. A Systematic Review On The Long-Term Success Of Calcium Phosphate Plasma-Spray-Coated Dental Implants. *Odontology*, 104, 347-56.
- Vohra, F., Al-Rifaiy, M. Q., Almas, K. & Javed, F. 2014. Efficacy Of Systemic Bisphosphonate Delivery On Osseointegration Of Implants Under Osteoporotic Conditions: Lessons From Animal Studies. *Arch Oral Biol*, 59, 912-20.
- Yuan, Y., Chesnutt, B. M., Wright, L., Haggard, W. O. & Bumgardner, J. D. 2008. Mechanical Property, Degradation Rate, And Bone Cell Growth Of Chitosan Coated Titanium Influenced By Degree Of Deacetylation Of Chitosan. *Journal Of Biomedical Materials Research Part B: Applied Biomaterials*, 86b, 245-252.